INTERNATIONAL JOURNAL FOR NUMERICAL METHODS IN FLUIDS
Int. J. Numer. Meth. Fluids 2003; **42**:1237–1248 (DOI: 10.1002/fld.592)

Influence of injection gate definition on the flow-front approximation in numerical simulations of mold-filling processes

Dhiren Modi, Pavel Šimáček and Suresh Advani*,†

Center for Composite Materials and Department of Mechanical Engineering, University of Delaware, Newark, DE 19716, U.S.A.

SUMMARY

Flow through porous media has been used to model resin impregnation in composites manufacturing processes such as resin transfer molding. Many numerical schemes have been used to explore the efficiency and accuracy in description of the movement of the liquid front when it is introduced through injection gates into a mold containing stationary and compacted fibrous porous media. In all numerical schemes, injection gates are modelled with a single node. Mathematically, a single node definition for a finite radius injection gate imparts a singularity. In this paper, an approach to avoid this singularity by modelling the injection gate with more than one node is presented. An analytical solution relating the fill time to the injection gate radius is developed for a constant pressure injection from a spherical injection gate into an isotropic media. A new parameter 'mesh density level', defined as the ratio of the injection radius to the element size, is used to investigate the accuracy and the convergence of the numerical results. It is shown that the numerical results converge when the mesh density level is increased. The accuracy of the results depends on the ratio of the flow-front radius to the injection gate radius as well as on the mesh density level. In many situations, a spherical injection gate may not represent the correct physics and model simplification may be necessary.

The impact of such simplifications is also quantified. The systematic analysis presented in this paper should prove useful to the modeller in taking the decision whether to select the proper, geometric definition for the injection gate to obtain accurate results or to define the injection gate using a single node and be aware of the errors introduced due to the singularity. Copyright © 2003 John Wiley & Sons, Ltd.

KEY WORDS: mold filling; radial injection; liquid composite molding; injection gate; flow-front; singularity; fibrous porous media

INTRODUCTION

Flow through porous media is encountered in many applications such as ground-water flow and liquid composite molding processes such as resin transfer molding (RTM) and vacuum

*Correspondence to: S. Advani, Center for Composite Materials and Department of Mechanical Engineering, University of Delaware, 126 Spencer Laboratory, Newark, DE 19716, U.S.A.
† E-mail: advani@me.udel.edu

Received 2 October 2002
Revised 5 May 2003

assisted resin transfer molding (VARTM) [1, 2]. The RTM process has become popular because of an ability to control the fibre reinforcement in the final part and manufacture complex shapes. In the RTM process, the fibre preform is placed into a mold cavity, the mold platens are closed together and the resin is injected from an injection gate under constant pressure or constant flow rate [2]. The success of the RTM process depends on the complete filling of the regions between the fibres in the mold cavity before the resin starts to cure and solidify [3, 4]. An understanding of the impregnation process helps the mold designer to understand the influence of the location of the injection gates and vents on the fibre impregnation and to ensure complete filling. Important output parameters are: the mold-filling time, the flow-front shape and the pressure distribution in the resin [5, 6].

Darcy's law [7] can be used to describe the mold-filling process [1–4] (Equation (1)):

$$\bar{U} = -\frac{\bar{K}}{\eta}\nabla p \tag{1}$$

Here, $\bar{U}$ is the macroscopic resin velocity vector, $\bar{K}$ is the permeability tensor of the porous media, η is the viscosity of the fluid and ∇p is the pressure gradient in the fluid. Invoking mass conservation of incompressible fluid in a stationary porous media and substitution of Equation (1) in the continuity equation, results in the following governing equation:

$$\nabla \cdot \left(\frac{\bar{K}}{\eta}\nabla p\right) = 0 \tag{2}$$

Typical RTM parts have a thickness of less than half an inch and so practice has focused on simplifying the models by treating RTM as a two-dimensional process. However, the increased demand for thicker parts, as well as parts having varying properties in the thickness direction, make it necessary to model these parts in three dimensions. Much of the literature available for modelling in three dimensions covers the development of numerical schemes for accurate simulations [8–16]. Lin [17, 18], Trochu [19] and Mohan [20–22], all used finite-element method, while Trochu [23] used boundary-fitted finite-difference method to simulate the mold-filling process. Chang [24] discussed adaptive re-meshing method for the RTM process simulations. Various other schemes such as boundary element, as well as implicit and explicit finite-element/control-volume method, have been employed, but as the modelling of impregnation of the fluid into porous media involves a moving boundary, the finite-element/control-volume (FE/CV) scheme to simulate the filling process has served well to capture the physics efficiently [25–27]. The solution domain is meshed with a fixed finite-element mesh. Control volumes are associated with each mesh node or alternatively with each element (Figure 1(a)). Each control volume has a fill factor associated with it, which ranges between zero (empty CV) and one (filled CV), and designates how much of the porous volume is already filled with the fluid (Figure 1(b)). The pressure in the empty control volumes is known to be equal to that of the vent, and the pressure in the filled control volumes is evaluated by the finite-element method, using Equation (2). Then, the flow Q_{ij}, between individual control volumes i and j, is determined from Equation (3) using the computed pressure field (Figure 1(c)).

$$Q_{ij} = \int_{s_{ij}} \mathbf{n}_i \cdot \frac{\mathbf{K}}{\eta}\nabla p \tag{3}$$

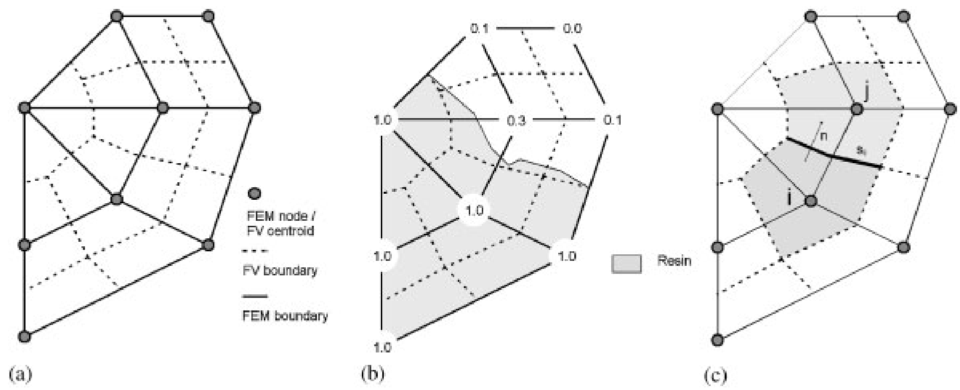

Figure 1. Finite-element/control-volume scheme for mold-filling process simulation: (a) domain discretization; (b) flow-front and fill factors; and (c) flow between control volumes.

Once the flow rates are known, flow is advanced by explicit integration in the time domain. The time step is selected so as to fill at least one additional control volume. This changes the fluid domain, and hence the boundary conditions. The pressure solution is sought for the new domain and this process is repeated until the complete porous media is saturated.

In most RTM processes, resin is injected from a gate of finite radius causing a three-dimensional flow. This gate in simulations is modelled using a single node. In explicit FE/CV approach, the pressure distribution is approximated using a finite-element scheme, while the flow-front progression is calculated from control-volume scheme. Thus, the injection gate size is a function of the element sizes containing the node representing the injection gate [28–30]. For constant pressure injection, the size of the gate and the numerical description of the gate will influence the accuracy of the resulting movement of the fluid in the porous media. Trochu [31] used finite-element method to simulate the flow through porous media and suggested to use refined mesh near the injection gate to accurately calculate the resin flow inside the mold. However, no results characterizing the influence of the element size near the injection gate as well as the geometric definition of the injection gate on the accuracy of the numerical results were reported. To investigate this effect, a case study of resin flow in a spherical mold (as an analytic solution is available), with two distinctly different-sized injection gates (0.01 and 0.005 m) and two different mesh density levels (0.707 and 1.306) (Equation (4)), was carried out (Figure 2). All the models were discretized with identical linear tetrahedron elements and the constant pressure injection gate was modelled with a single node.

$$\text{Mesh density level} = \frac{\text{Injection radius size}}{\text{Element size}} \tag{4}$$

$$\text{Relative error (\%)} = \frac{\text{Analytical solution} - \text{Numerical solution}}{\text{Analytical solution}} \tag{5}$$

The results show that as the mesh density level increases, the error (Equation (5)) in the approximated flow-front radius as compared to the analytical flow-front radius (Equation (15)) increases. Also, the error depends on the ratio of the flow-front radius to the injection gate

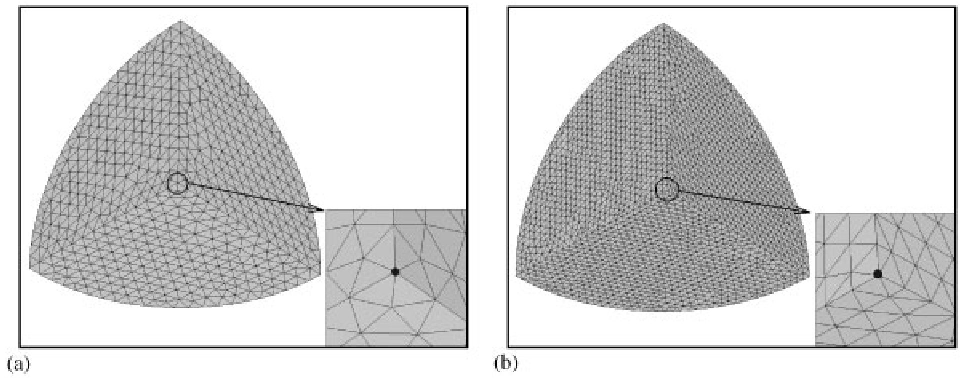

Figure 2. Three-dimensional models used to investigate the influence of various mesh density levels on the approximation of the flow-front radius, when the injection radius is defined with a single node.

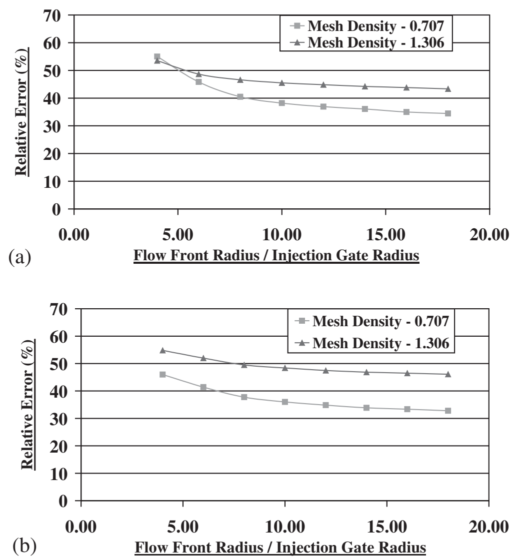

Figure 3. Relative error in the approximated flow-front radius for constant pressure injection using three-dimensional models discretized with two different mesh density levels. The injection radius is defined with a single node: (a) injection radius size -0.01 m; and (b) injection radius size -0.005 m. In both the cases, the error increases as the mesh density level is increased.

radius (Figure 3). Thus, as the mesh size is refined, we tend to model the mathematical singularity imposed by a single node injection and the numerical results diverge from the analytical solution for a finite injection radius.

The above study used point injection, and to achieve accurate results, it was necessary to use the elements near the injection gate of a particular size only. For higher accuracy, or for cases in which reasonable accuracy is desired with a coarser mesh, the approach fails to offer any flexibility. Therefore, it is necessary to avoid this mathematical singularity by modelling the injection gate with more than one node. No reported work is available to estimate the accuracy and the convergence of such numerical results. This paper investigates the accuracy and the convergence of the numerical results, when the injection gate is modelled with more than one node to avoid the mathematical singularity.

ANALYTICAL SOLUTION

An analytical solution for a three-dimensional mold-filling process with a two-dimensional injection gate is difficult to develop. However, due to a high resin viscosity, a flow-front instantaneously develops into a spherical shape. Thus, the injection gate can be assumed to be of a spherical shape and an analytical solution can be derived relating the flow-front radius to the injection radius, the injection pressure and the time to fill a spherical mold of radius R (Figure 4).

Conservation of the mass of resin flowing inside a mold can be expressed in terms of velocities in r, θ and φ, directions, using a spherical co-ordinate system as follows:

$$\frac{1}{r^2}\frac{\partial}{\partial r}(r^2 U_r) + \frac{1}{r\sin\theta}\frac{\partial}{\partial\theta}(U_\theta \sin\theta) + \frac{1}{r\sin\theta}\frac{\partial U_\varphi}{\partial\varphi} = 0 \tag{6}$$

Using the symmetry in the flow in θ and φ directions and Darcy's law, the pressure gradient in the radial direction can be found from Equation (6) as

$$\frac{\mathrm{d}p}{\mathrm{d}r} = -\frac{\phi\eta}{K}\frac{C_1}{r^2} \tag{7}$$

To find the pressure distribution in the part, we need to integrate Equation (7) with the following boundary conditions:

$$At\, r = r_0, \quad p = p_{\mathrm{inj}} \tag{8}$$

$$At\, r = R, \quad p = p_f = 0 \tag{9}$$

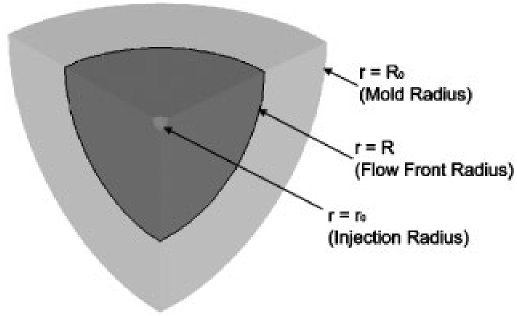

Figure 4. Hemispherical section of a mold showing resin injection from a spherical gate into a spherical mold and flow-front progression. Injection is under constant pressure boundary condition.

This gives the pressure distribution in the resin as

$$p(r) = \frac{r_0}{(R - r_0)} (p_{\text{inj}}) \left(\frac{R}{r} - 1 \right) \tag{10}$$

Note that due to a mathematical singularity, r_0 cannot be zero. The pressure gradient at the flow-front radius can be determined by taking the derivative of the pressure solution (Equation (10)) with respect to radius and setting $r = R$ (the flow-front radius).

$$\left. \frac{\mathrm{d}p}{\mathrm{d}r} \right|_{r=R} = \frac{-r_0}{(R - r_0)} (p_{\text{inj}}) \frac{1}{R} \tag{11}$$

The flow-front velocity corresponds to the time gradient of the flow-front radius. From Equation (11), we can write

$$U_r \bigg|_{\text{at}(r=R)} = \frac{\mathrm{d}R}{\mathrm{d}t} = -\frac{K}{\phi\eta} \frac{\mathrm{d}p}{\mathrm{d}r} \bigg|_{\text{at}(r=R)} = \frac{K}{\phi\eta} \frac{r_0}{(R - r_0)} (p_{\text{inj}}) \frac{1}{R} \tag{12}$$

Using the separation of variables method and integrating the resulting equation with the following boundary conditions (Equation (13) and (14)):

At the start of the solution ($t = 0$), the flow – front radius is the same as the injection radius ($R = r_0$) and (13)

At the current time ($t = t$), the flow – front has reached a radius $R(R = R)$ (14)

the relation between the flow-front radius and the fill time, t, can be found as

$$2 \left(\frac{R}{r_0} \right)^3 - 3 \left(\frac{R}{r_0} \right)^2 + 1 = \frac{6K(p_{\text{inj}})t}{\phi\eta r_0^2} \tag{15}$$

Similar analysis for a radial flow in a two-dimensional mold with resin injection from a two-dimensional injection gate shows that the singularity is weaker in this case (Equation (16)):

$$\left(\frac{R}{r_0} \right)^2 \left(2 \ln \left(\frac{R}{r_0} \right) - 1 \right) + 1 = \frac{4K(p_{\text{inj}})t}{\phi\eta r_0^2} \tag{16}$$

NUMERICAL SIMULATIONS

In order to check the accuracy of the numerical results, a spherical mold domain with a spherical injection gate of size 0.01 m was discretized using an equal-sized linear tetrahedron elements as shown in Figure 5. The mesh density levels were kept the same as in the previous analysis and constant pressure injection boundary condition was imposed at all nodes on the injection radius. Other parameters used in the analysis are listed in Table I. The numerical flow-front radius at different times was determined and compared with the analytical solution (Equation (15)). By the nature of the singularity, the error in the flow-front radius

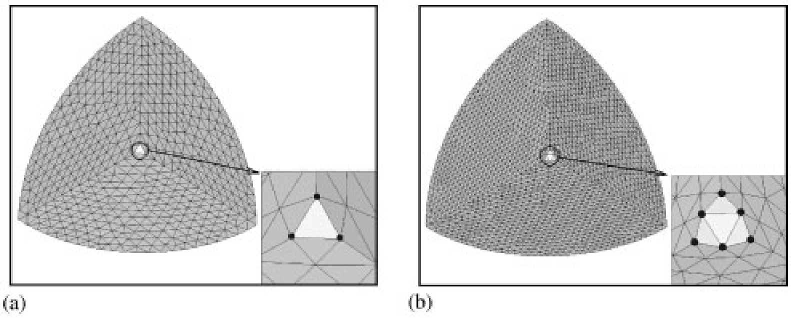

Figure 5. Three-dimensional models with a spherical injection radius modelled with more than one node to investigate the influence of the mesh density ratio on the approximation of the flow-front radius. Constant pressure injection boundary condition is imparted at all nodes on the spherical injection radius.

Table I. Material and process parameters used in the mold-filling simulations.

Permeability (Isotropic)	1E-10 m^2
Resin viscosity	1 Pa s
Injection pressure	101 300 Pa
Fibre volume fraction	0.5

approximation can be expected to be higher in the vicinity of the injection radius and hence the study was limited until the flow-front radius was 20 times that of the injection radius. For the convergence analysis, the mesh density level was increased and the results were benchmarked with the analytical solution. To further check the effect of the injection gate size, a different-sized spherical injection gate (0.005 m) was modelled with same mesh density levels and the numerical results from these models were compared with the analytical solution.

From the viewpoint of using the numerical schemes, there are many approaches of modelling the injection gate. The most accurate approach is to model the spherical-shaped injection gate, which is time consuming. Other simplified but approximate approaches include defining those nodes within the distance of injection radius as gates or injecting from a two-dimensional injection gate. For example, four nodes on a face of a brick element can be used to define a two-dimensional injection gate (Figure 6). A rigorous comparison of the results from the models with this type of approximately defined injection radius, with the results from the models with an accurately defined injection radius is inappropriate, due to the different injection radius definitions and the element types. However, due to the assumption of a high resin viscosity and a fully developed flow-front, we can still compare the numerical results with the analytical solution derived for the spherical injection. The error margin one can expect in such modelling simplifications of the injection gate is also estimated.

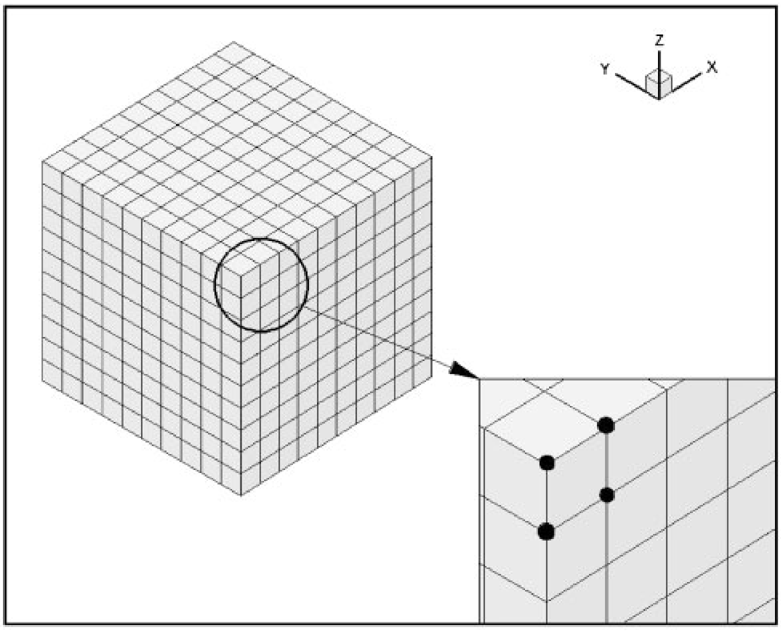

Figure 6. Three-dimensional mesh of a mold domain. Mesh density ratio is kept equal to one and a circular injection gate is defined with four nodes of an element.

RESULTS AND DISCUSSION

As shown in Figure 7(a), when the spherical injection gate of 0.01 m radius was modelled using a spherical surface, the numerical results had considerable error (Equation (5)) for the low ratios of the flow-front radius to the injection radius.

As this ratio becomes large (>5), the error reduced. Consequently, low mesh density level may not be sufficient if one wants to model the flow in the vicinity of the injection gate accurately. Figure (7a) also shows the numerical results from a model with an increased mesh density level. The results exhibit a clear convergence i.e. the accuracy in approximation of the flow-front radius improves for all ratios of the flow-front radius to the injection gate radius, especially for smaller ratios (<5).

The numerical results from the models with different injection radius size (0.005 m), and same mesh density levels, exhibit the same behaviour and the same error margins (Figure (7b)).

The following reasons can be cited for this improvement. When the injection radius is defined with a single node, the pressure approximation starts from this nodal location instead of the actual injection location. In addition, the flow area for the resin flow from the injection gate into the mold is calculated from the area of the faces of the control volume associated with the injection node. With successive increase in mesh density, this control volume as well as the area of the associated faces also decreases. These erroneous pressure approximation as well as an unbound reduction in the flow area with increase in the mesh density leads to a large error in the approximated flow-front radius (Figure (8a) and (8b)).

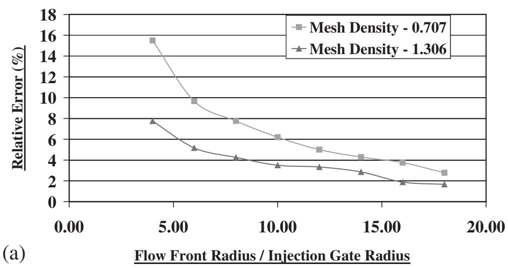

(a)

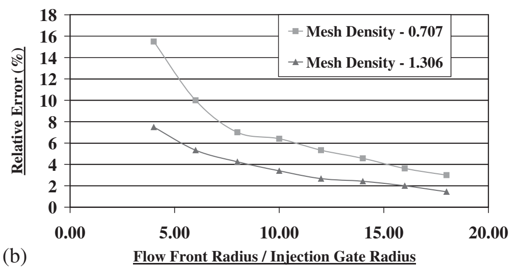

(b)

Figure 7. Relative error in the approximated flow-front radius from the three-dimensional models discretized using two different mesh density levels. Constant pressure injection boundary condition is imparted at all nodes on the injection radius. (a) Injection radius size = 0.01 m; and (b) injection radius size = 0.005 m. In both cases, the error decreases as the mesh density level or flow-front radius to injection radius ratio is increased.

With the properly defined injection radius, the pressure approximation starts from the correct injection location and hence, solely depends on the mesh density level i.e. the number of nodes used to model the spherical injection surface and the number of nodes/elements inside the domain. The properly modelled injection radius leads to an accurate representation of the actual spherical surface area for resin flow. The subsequent increase in the mesh density, in this case also, leads to a reduced resin flow area. However, the reduction is bound at the lower limit by the spherical injection radius size. Thus, properly defined injection radius enables one to approximate the pressure distribution and the resin flow area accurately leading to an accurate resin flow rate and fill times (Figure (8c)).

Figure 9 shows the numerical results from a three-dimensional model with a mesh density ratio of one and an injection radius defined with four nodes on a face of a brick element. From Equation (15), it can be seen that the accuracy of the results is acceptable.

CONCLUSION

It has been shown that the constant pressure injection gate definition with a single node in the explicit FE/CV method for RTM mold-filling simulations is erroneous as it imparts a mathematical singularity. It is necessary to model the injection gate with more than one node for numerical convergence. The instantaneous development of the flow-front into a spherical shape at the injection gate due to high resin viscosity, allows us to assume a spherical injection gate and derive the analytical solution for a spherical injection and investigate the accuracy

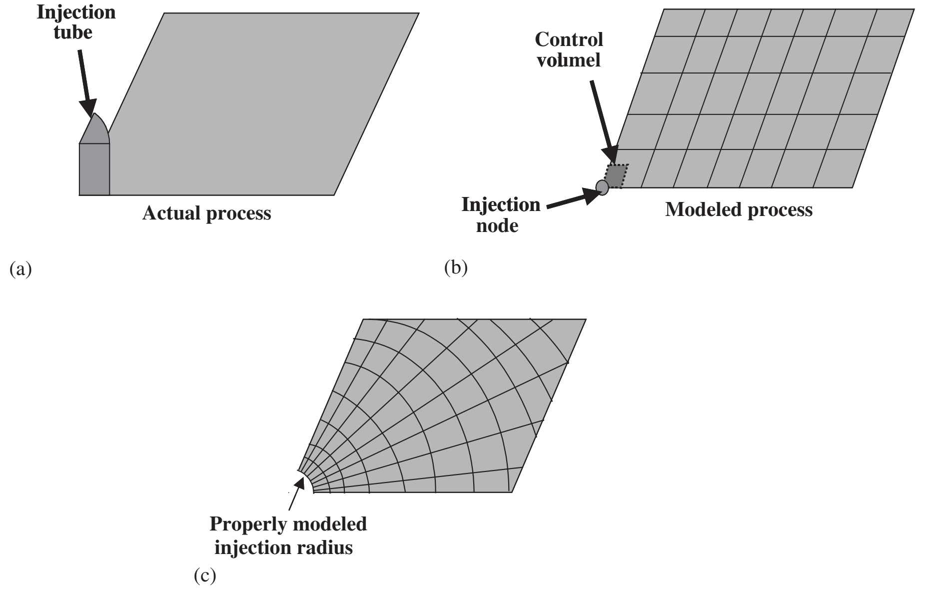

Figure 8. (a) The actual process conditions involve injection from a finite-sized injection radius; (b) injection radius modelling with a single node leads to incorrect pressure approximation and incorrect flow area. Successive increase in the mesh density level gives an unbound reduction in the flow area, responsible for the non-convergent behaviour of the results; and (c) with proper modelling of the injection radius, the pressure boundary conditions are imposed at the correct location. The flow area reduction is bounded on the lower limit by the injection radius size. Successive increase in the mesh density level gives improved pressure approximation and convergent results.

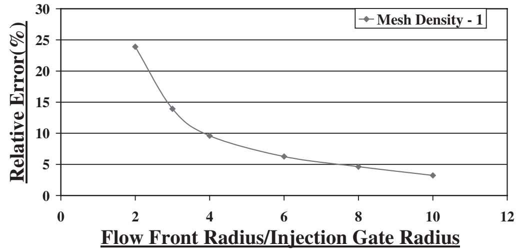

Figure 9. Relative error in the approximated flow-front radius from the three-dimensional models discretized using brick elements. The mesh density level is one and the injection radius is defined with the four nodes on a face of the element.

and the convergence of the numerical results. It was found that for a spherical injection, the error in the approximation of the flow-front radius depends on the mesh density level and the ratio of the flow-front radius size to the injection radius size. In many cases, when there are multiple gates through which resin enters the mold, it may not be suitable or practical to describe a spherical surface at each injection gate. Hence, model simplification may be welcome. Investigation of the use of a two-dimensional injection gate shows reasonable accuracy. Hence, it is recommended to use proper geometric definition for the injection gate, wherever possible. If proper modelling of the injection gate is not possible, the injection gate should be modelled using all the nodes at a distance less than or equal to the injection radius. In extreme cases, where only one node is positioned within the injection radius, it is permissible to define the injection gate using a single node. The results from such models should be analysed with extra precaution.

NOMENCLATURE

r_0	injection gate radius
R	flow-front radius
R_0	mold radius
∇p	pressure gradient
p_{inj}	injection pressure (Constant)
p_f	flow-front pressure (0 in our case)
$\bar{U}$	macroscopic resin velocity vector
U_r, U_θ, U_φ	flow-front velocity in spherical co-ordinates
$\langle U_r \rangle$	volume averaged resin velocity in radial direction
$\bar{K}$	permeability tensor
K	permeability (Isotropic)
η	resin viscosity
ϕ	porosity

REFERENCES

1. Bear J. *Dynamics of Fluids in Porous Media*. Elsevier: New York, 1972.
2. Advani SG. *Flow and Rheology in Polymer Composites Manufacturing*. Elsevier: New York, 1994.
3. Scheidegger AE. *The Physics of Flow Through Porous Media*. University of Toronto Press: New York, 1974.
4. Bruschke M. A predictive model for permeability and non-isothermal flow of viscous and shear-thinning fluids in anisotropic fibrous media. *Ph.D. Thesis*, University of Delaware, Newark, Delaware, 1993.
5. Bickerton S. Important mold filling issues in liquid composites molding processes: modeling and experiments. *Proceedings of the Annual Meeting of the Society of Plastics Engineers: ANTEC 97*, Ontario, 1997.
6. Bruschke MV, Advani SG. RTM: filling simulation of complex three-dimensional shell-like structures. *SAMPE Quarterly* 1991; **23**(1):2–11.
7. Darcy H. *Les Fontaines Publiques de la Ville de Dijon*. Dalmont: Paris, 1856.
8. Patel N, Lee LJ. Modeling of void formation and removal in liquid composite molding. Part I: Wet ability analysis. *Polymer Composites* 1996; **17**(1):96–103.
9. Patel N, Lee LJ. Modeling of void formation and removal in liquid composite molding. Part II: Model development and implementation. *Polymer Composites* 1996; **17**(1):104–114.
10. Lee B, Springer. Model for determining the vent locations and the fill time of resin transfer molds. *Journal of Composite Materials* 1995; **29**(3):306–333.
11. Li S, Gauvin R. Numerical analysis of the resin flow in resin transfer molding. *Journal of Reinforced Plastics and Composites* 1991; **10**(3):314–327.
12. Young WB. Analysis of resin injection molding in molds with preplaced fiber mats: 2.Numerical simulation and experiments of mold filling. *Polymer Composites* 1991; **12**(1):30–38.
13. Voller VR, Chen YF. Prediction of filling time in porous cavities. *International Journal for Numerical Methods in Fluids* 1996; **23**(7):661–672.
14. Young WB, Han K, Fong LH, Lee LJ, Liou MJ. Flow simulation in molds with preplaced fiber mats. *Polymer Composites* 1991; **12**(6):391–403.
15. Mohan RV, Shires DR, Tamma KK, Ngo ND. Flow channels/fiber impregnation studies for the process modeling/analysis of complex engineering structures manufactured by resin transfer molding. *Polymer Composites* 1998; **19**(5):527–542.

16. Coulter JP. Resin impregnation during the manufacturing of composite materials. *Ph.D. Thesis*, University of Delaware, Newark, Delaware, 1987.
17. Lin M, Huh H, Hahn HT. A finite element simulation of resin transfer molding based on partial nodal saturation and implicit time integration. *Composites part A: Applied Science and Manufacturing* 1998; **29**(5–6):541–550.
18. Lin Y. A finite element simulation of resin transfer molding. *Ph.D. Thesis*, University of California, Los Angeles, 1998.
19. Trochu F, Gauvin R, Gao DM. Numerical analysis of the resin transfer molding process by the finite element method. *Advances in Polymer Technology* 1993; **12**(4):329–342.
20. Mohan RV, Ngo ND, Tamma KK. On a pure finite element based Methodology for resin transfer mold filling simulations. *Polymer Engineering and Science* 1999; **39**(1):26–43.
21. Mohan RV, Ngo ND, Tamma KK. Three-dimensional resin transfer molding: isothermal process modeling and implicit tracking of moving fronts for thick, geometrically complex composites manufacturing applications—part 2. *Numerical Heat Transfer, Part-A: Applications* 1999; **35**(8):839–858.
22. Mohan RV, Ngo ND, Tamma KK, Fickie KD. Process modeling and implicit tracking of moving fronts for three-dimensional thick composite manufacturing. *Paper* AIAA-96-0725, Aerospace Science Meeting, Reno, 1996.
23. Trochu F, Gauvin R. Limitations of a boundary-fitted finite difference method for the simulation of the resin transfer molding process. *Journal of Reinforced Plastics and Composites* 1992; **11**(7):772–786.
24. Chang W, Kikuchi N. An adaptive remeshing method in the simulation of Resin Transfer Molding (RTM) process. *Computer Methods in Applied Mechanics and Engineering* 1994; **112**(1–4):41–68.
25. Tucker C. *Fundamentals of Computer Modeling for Polymer Processing*. Hanser: New York, 1989.
26. Cai Z. Simplified mold filling simulation in resin transfer molding. *Journal of Composite Materials* 1992; **26**(17):2606–2630.
27. Lin Y, Murphy MJ, Hahn HT. Resin transfer molding process optimization. *Composites part A: Applied Science and Manufacturing* 2000; **31**(4):361–371.
28. Advani SG, Simacek P. *LIMS-5.0 User Manual*. Center for Composite Materials, Newark, Delaware, 2000.
29. Fracchia CA, Castro J, Tucker C. A finite element/control volume method for simulation of resin transfer mold filling. *Proceedings of American Society for Composites*, Lancaster, PA, 1989; 157–166.
30. Bruschke MV, Advani SG. A finite element/control volume approach to mold filling in anisotropic porous media. *Polymer Composites* 1990; **11**(6):398–405.
31. Francois T, Gauvin R, Ming GD, Boudreault J. RTM-FLOT—An integrated software environment for the computer simulation of the resin transfer molding process. *Journal of Reinforced Plastics and Composites* 1994; **13**(3):262–270.

